Peri-renal adipose inflammation contributes to renal dysfunction in a non-obese prediabetic rat model: Role of anti-diabetic drugs

Safaa H. Hammoud [a], Ibrahim AlZaim [b,c], Nahed Mougharbil [b], Sahar Koubar [d], Ali H. Eid [e,f], Assaad A. Eid [g,*], Ahmed F. El-Yazbi [b,h,i,*]

[a] Department of Pharmacology and Therapeutics, Faculty of Pharmacy, Beirut Arab University, Beirut, Lebanon
[b] Department of Pharmacology and Toxicology, Faculty of Medicine, The American University of Beirut, Beirut, Lebanon
[c] Department of Biochemistry and Molecular Genetics, American University of Beirut, Beirut, Lebanon
[d] Division of Nephrology, Department of Internal Medicine, Faculty of Medicine, The American University of Beirut, Beirut, Lebanon
[e] Department of Basic Medical Sciences, College of Medicine, Qatar University, Doha, Qatar
[f] Biomedical and Pharmaceutical Research Unit, QU Health, Qatar University, Doha, Qatar
[g] Department of Anatomy, Cell Biology, and Physiological Sciences, Faculty of Medicine, The American University of Beirut, Beirut, Lebanon
[h] Department of Pharmacology and Toxicology, Faculty of Pharmacy, Alexandria University, Alexandria, Egypt
[i] Faculty of Pharmacy, Alalamein International University, Alalamein, Egypt

ARTICLE INFO

ABSTRACT

Diabetic nephropathy is a major health challenge with considerable economic burden and significant impact on patients' quality of life. Despite recent advances in diabetic patient care, current clinical practice guidelines fall short of halting the progression of diabetic nephropathy to end-stage renal disease. Moreover, prior literature reported manifestations of renal dysfunction in early stages of metabolic impairment prior to the development of hyperglycemia indicating the involvement of alternative pathological mechanisms apart from those typically triggered by high blood glucose. Here, we extend our prior research work implicating localized inflammation in specific adipose depots in initiating cardiovascular dysfunction in early stages of metabolic impairment. Non-obese prediabetic rats showed elevated glomerular filtration rates and mild proteinuria in absence of hyperglycemia, hypertension, and signs of systemic inflammation. Isolated perfused kidneys from these rats showed impaired renovascular endothelial feedback in response to vasopressors and increased flow. While endothelium dependent dilation remained functional, renovascular relaxation in prediabetic rats was not mediated by nitric oxide and prostaglandins as in control tissues, but rather an upregulation of the function of epoxy eicosatrienoic acids was observed. This was coupled with signs of *peri*-renal adipose tissue (PRAT) inflammation and renal structural damage. A two-week treatment with non-hypoglycemic doses of metformin or pioglitazone, shown previously to ameliorate adipose inflammation, not only reversed PRAT inflammation in prediabetic rats, but also reversed the observed functional, renovascular, and structural renal abnormalities. The present results suggest that *peri*-renal adipose inflammation triggers renal dysfunction early in the course of metabolic disease.

1. Introduction

Diabetes mellitus is one of the leading non-communicable diseases associated with high mortality rates [1]. Diabetic complications could result in life-threatening disorders in multiple organ systems [2]. The development and prevalence of diabetes and its complications are influenced by several risk factors. Among these complications, chronic kidney disease (CKD) is a main health challenge worldwide [3,4]. Diabetic nephropathy initiates as hyperfiltration followed by a gradual decline in renal function culminating in end-stage kidney disease [5].

Clinical practice guidelines recommend tight glycemic control to reduce the progression of diabetic complications, with tighter targets advised for patients with nephropathy [6]. However, intensive hypoglycemic therapy was found to be ineffective in altering the progression

of CKD to end-stage kidney disease in diabetic patients [7]. Moreover, the metabolic syndrome, occurring in the course of type 2 diabetes, was shown to induce CKD, implicating factors other than hyperglycemia and hypertension in the diabetic renal involvement [8–10]. In parallel, clinical studies addressing vascular complications in diabetic patients revealed that lowering glucose levels was insufficient to reduce risks of those complications [11,12]. As well, the fact that CKD is often detected early in the course of type 2 diabetes and the evidence of vascular complications in prediabetic patients pose the question of the nature of factors instigating early renal and vascular dysfunction in the initial stages of metabolic impairment [12].

Previous reports highlighted a role for inflammation in diabetic vascular diseases apart from hyperglycemia [13,14]. Indeed, the tight link between obesity and CKD led to the assumption that adipose tissue expansion, which promotes inflammation and oxidative stress, may be involved in alteration of renovascular function [8,14]. Inflammation associated with visceral obesity contributes to endothelial dysfunction in many patients with prediabetes [15]. Yet, specific studies to address the exact pathway leading to renal injury or whether early elimination of risk factors could delay or even prevent adverse outcomes were not addressed. Similarly, the mechanistic framework through which early metabolic challenge induces kidney disease has not been thoroughly explored.

Being asymptomatic in nature, the diagnosis of the earliest stages of CKD is challenging, particularly because it is difficult to unequivocally define the onset of metabolic changes [16]. Indeed, our previous work on a rat model of mild hypercaloric intake (HC) leading to a non-obese prediabetic phenotype of metabolic impairment showed that significant cardiovascular, cerebrovascular, vascular endothelial, cardiac autonomic, and cognitive dysfunction occur in the absence of obesity, hyperglycemia, or hypertension [17–21]. The earliest signs of metabolic impairment seen consistently in this model were altered body composition, hyperinsulinemia, and localized perivascular adipose inflammation. This rat model degenerated into *bona fide* type 2 diabetes with hyperglycemia and elevated glycosylated hemoglobin levels upon prolonged HC feeding [17,20]. Significantly, interventions ameliorating perivascular adipose tissue inflammation, namely the antidiabetic drugs metformin and pioglitazone, corrected the observed vascular, hemodynamic, autonomic, and cognitive alterations mostly with no effect on metabolic parameters.

In the present study, we hypothesize that early metabolic dysfunction associated with adipose inflammation in this model is also associated with renal impairment that is driven by renovascular alterations. We show that perirenal adipose tissue (PRAT) inflammation might contribute to a state of hyperfiltration via loss of proper renovascular endothelial control. This was coupled with mild to moderate changes in renal oxidative stress, histopathology, and inflammation. Intervention with either metformin or pioglitazone appeared to correct these changes.

2. Materials and methods

2.1. Experimental animals

All animal studies were conducted according to a protocol approved by the Institutional Animal Care and Use Committees of the American University of Beirut and in accordance with the Guide for Care and Use of Laboratory Animals. Male Sprague-Dawley rats (5–6 weeks of age; 150 g) were used in this study. Rats were housed individually and had unrestricted access to food and water throughout the study. Male rats were randomly allocated to four groups ($n = 6$ each), and fed (1) normal chow (control, NC, Envigo, Teklad Rodent Diets, Madison, WI, 3 Kcal/g), (2) HC diet for 12 weeks (HC, 4.035 Kcal/g), (3) HC diet for 12 weeks and treated with Metformin (Met, 30 mg/kg twice daily), and (4) HC diet for 12 weeks and treated with Pioglitazone (Pio, 2.5 mg/kg daily). An additional group of five rats fed HC diet for four weeks was added to

examine whether the renal functional and structural alteration occurred as a direct consequence of dietary exposure prior to the development of the metabolic changes characteristic of adipose inflammation. The metabolic parameters in these rats were compared to age matched control rats.

HC diet was prepared as previously described [17–21]. Rats were caged individually, daily food intake was recorded, and calorie intake was calculated. During the last 2 weeks of HC feeding, rats in designated treatment groups received oral treatment with either pioglitazone or metformin incorporated into the chow as described previously [17,20]. The doses selected were commonly used in the literature to produce *in vivo* cardiovascular and renal protective actions without a hypoglycemic effect [22–24]. In our previous work, these doses were shown to lack an effect on weight gain, fasting and random blood glucose levels, glycosylated hemoglobin levels, serum advanced glycated end products, or serum lipid levels. As well, these doses consistently demonstrated an anti-inflammatory effect on adipose tissue and improved cardiovascular function in prediabetic rats without altering any of the aforementioned parameters [17,18,20,25].

2.2. Non-invasive blood pressure measurement and examination of body composition:

Following the intended feeding duration, systolic blood pressure was measured non-invasively by tail cuff using CODA High Throughput Monitor (Kent Scientific, Torrington, CT) [26]. Any irregular or unacceptable recording noted as a false recording by the system was excluded. On the other hand, LF10 Minispec Nuclear Magnetic Resonance (NMR) machine (Bruker, MA, USA) was used to measure rat fat: lean ratio to detect different tissue densities. The values obtained from each rat were compared to a standardized, calibrated rat.

2.3. Urine and serum collection and analysis

Following the designated feeding and treatment duration, animals were housed in metabolic cages, in which urine was collected. Serum was also collected from fasted rats for creatinine, blood glucose and lipid profile measurements. Twenty four-hour urine was collected and centrifuged at 6,000 g for 15 min. The supernatant was stored at $-20\,°C$ until its use for protein and creatinine measurement. Overnight fasted rats were anesthetized with thiopental sodium (50 mg/kg); blood samples were collected from the orbital plexus, spun at 4000 rpm for 10 min. The serum was aspirated and stored at $-20\,°C$ until its use for biochemical analyses. Insulin levels in serum were assessed using a rat insulin ELISA kit (Thermo-Fisher Scientific, Waltham, MA). Measurement of blood glucose was done using Accu-check Performa glucometer (Roche Diagnostics, Rotkreuz, Switzerland). Creatinine levels in blood and urine, and serum triglyceride were carried out using Fluitest assay kits (Biocon Diagnostik, Mönchberg, Germany) according to the manufacturer's protocol. Glomerular filtration rate (GFR) was calculated from creatinine concentrations in blood and urine with respect to volume of urine in 24 h. Total protein concentration in urine was determined using the Bradford assay [27].

2.4. Tissue collection and renovascular experiments

Following the overnight fasting, urine and serum collection, the left kidney of the anesthetized rats was isolated and perfused according to the method described previously [28]. Briefly, the left kidney was exposed by an abdominal incision. The renal artery was catheterized with an 18-gauge needle through a small incision made after aortic ligation. Immediately, the kidney was flushed with heparinized saline and was perfused with Krebs solution (NaCl 120, KCl 5, $CaCl_2$ 2.5, $MgSO_4·7H_2O$ 1.2, KH_2PO_4 1.2, $NaHCO_3$ 25, and glucose 11 mM) on a constant flow rate of 5 ml/min maintained at 37 °C and aerated with 95% O_2 and 5% CO_2. The constant flow was delivered using a peristaltic

pump (Model P3; Pharmacia Fine Chemicals, Sweden).

The pump delivered a pulsatile flow, and the venous effluent was allowed to drain freely. The kidney perfusion pressure was continuously monitored by means of a Millar pressure transducer distal to the pump and recorded on a LabChart-8 pro software (AD Instruments Ltd., Dunedin, New Zealand). At the beginning of the experiment, a stabilization period of 30 min was allowed. The perfusion rate was changed to 7.5 ml/min for few minutes to assess renal endothelial feedback. To study the endothelium-dependent vasodilation, the renal vascular tone was elevated by continuous infusion of the α1-adrenoreceptor agonist phenylephrine (PE, 10 μM). Endothelium-dependent relaxation was examined in response to increasing concentrations of carbachol (CCh, $1x10^{-12}$ M $- 1 \times 10^{-5}$ M) injected into the perfusion solution. CCh effect was represented as the percentage inhibition the PE-mounted pressure. The contribution of the typical components of endothelium-mediated relaxation was assessed by the addition of the corresponding inhibitors in the perfusion solution; N^{ω}-nitro-L-arginine (L-NAME, 100 μM) and diclofenac (7 μM). As well, the role of arachidonic acid derivatives, 20-Hydroxyeicosatetraenoic acid (20-HETE) and epoxyeicosatetraenoic acids (EETs) in the CCh-evoked relaxation was examined using HET0016 (1.5 μM, Cayman Chemicals, Ann Arbor, MI) and MSPPOH (12 μM, Cayman Chemicals, Ann Arbor, MI), being selective inhibitors of the renal microsomal enzymes producing 20-HETE [29] and EETs [30], respectively. The concentrations used were selected based on our prior experiments on isolated perfused kidney [28].

The right kidney was then removed. Renal cortices were dissected and PRAT was carefully collected from adipose tissues surrounding the kidney as described previously [31]. The tissues collected were alternated between snap freezing in liquid nitrogen and storage at $-80\,^{\circ}$C for molecular experiments or fixation in 4% formaldehyde, and then embedding in paraffin blocks for histology and immunostaining studies.

2.5. Immunofluorescence, immunohistochemistry and histopathology

Kidney sections (4 μm) of paraffin-embedded tissues were stained with periodic acid Schiff stain (PAS) or Masson's trichrome stain while those of the PRAT were stained with Hematoxylin & Eosin (H&E). PAS staining was used for the examination of glomerular and mesangial matrix area changes. Mesangial matrix index was calculated as the ratio of mesangial area to glomerular area × 100 (% area). Masson's trichrome staining was done for assessment of glomerulosclerosis. In each representative slide, trichrome staining was semi-automatically quantified in 20 fields and expressed as a percentage of staining of total surface area, and the results from all fields were averaged. H&E was used to assess adipocyte size measured by ImageJ. At least 10 adipocytes were measured from five random areas in the slide in question. Quantification was performed by a blinded assessor via isolation and quantification of the staining intensity using ImageJ software and normalization to the tissue area in each slide.

Immunohistochemical detection of α–smooth muscle actin (α-SMA) was performed using 1:500 concentrations of rabbit anti-α-SMA (Abcam, Cambridge, UK), and visualized using Novolink Polymer Detection Kit (Leica Biosystems, Buffalo Grove, Illinois) according to the manufacturer's protocol. Control experiments were performed by omitting primary antibodies and using rabbit IgG controls. Staining score was assessed by recording the number of tubules stained out of 100 counted tubules.

Indirect immunofluorescence analysis was used to identify a tubular epithelial marker, Cytokeratin. Paraffin-embedded tissues were deparaffinized and treated with a citrate antigen retrieval buffer (pH 6) for 40 min in a steamer. Sections were allowed to cool to room temperature and were then washed and incubated with protein blocking buffer (10% normal goat serum (NGS), 0.1% Triton X-100, 3% bovine serum albumin (BSA) in PBS) for 1 h to block non-specific sites. Sections were then washed twice with PBST (0.05% Tween-20 in PBS) and incubated with 1:100 rabbit anti-cytokeratin (Abcam, Cambridge, UK) in 2% NGS, 0.1%

Triton X-100, 3% BSA in PBS overnight at 4 °C in a humidified chamber. Slides were then washed twice with PBST and were incubated with 1:1000 secondary goat anti-rabbit Texas red antibody (Abcam, Cambridge, UK) in 2% NGS and 0.1% Triton X-100 in PBS at room temperature for two hours in the dark. Finally, slides were rinsed three times in PBST and were mounted. Ten random representative fields per tissue section were taken and the percentage area of 100 tubules per section along with the average pixel intensity per slide were compared among groups. Zen light software (2.3 blue version) was used for quantification of florescence intensity, and values were expressed as fluorescence intensity (arbitrary units) per tubule.

Reactive oxygen species load was detected using dihydroethidium staining (DHE) method as previously described [32]. Staining was performed on cryosections of PRAT and kidney cortices. Fluorescent images of ethidium-stained kidney tissue were obtained with a laser-scanning confocal microscope (Carl Zeiss, Germany) and were detected through the Alexa Fluor 568 filter for the DHE red fluorescent labeling indicating superoxide production. Six random areas per tissue section were taken, and the average pixel intensity for each animal was compared among groups. Zen light software (2.3 blue version) was used for quantification of fluorescence intensity, and values were expressed as fluorescence intensity (arbitrary units).

2.6. Western blot analysis

Western blotting was performed as described previously [17,32]. Kidney cortices and PRAT samples were homogenized on ice, and the protein extracts were separated by SDS-polyacrylamide gel electrophoresis. Proteins were then blotted to nitrocellulose membranes and were incubated in primary antibodies (1:1000 for rabbit polyclonal anti-phospho-eNOS Ser1177 and rabbit polyclonal anti-eNOS, 1:500 for rabbit polyclonal anti-IL-1β, 1:100 for rabbit anti-TGF-β1, 1:200 for rabbit monoclonal anti-VEGF, 1:500 for rabbit polyclonal anti-CYP2C11 and 1:1000 for rabbit monoclonal anti-GAPDH, rabbit polyclonal anti-hypoxia inducible factor 1α (HIF1-α), Abcam, Cambridge, UK, and rabbit polyclonal anti-uncoupling protein 1 (UCP1), Cellsignaling, Danvers, MA) overnight at 4C. Membranes were then washed with 0.02% TBST (Tris-buffered saline with 0.1% Tween 20) and incubated for 1 h at room temperature in 1:40,000 biotinylated conjugated goat anti-rabbit Ig. Membranes were then washed and incubated for 30 min at room temperature with 1:200,000 HRP-conjugated streptavidin (Abcam, Cambridge, UK). After two washes with 0.02% TBST (5 min) and two washes with TBS (5 min), the blots were exposed to Clarity Western ECL substrate (BioRad, Hercules, California) for 5 min and then detected by Chemidoc imaging system (BioRad, Hercules, CA). Densitometric analysis of the protein bands was performed using ImageJ software. Measurements were normalized to the density of total protein for p-eNOS after stripping and re-probing or GAPDH for IL-1β, TGF-β1, UCP1, HIF1-α, VEGF, and CYP2C as described previously.

2.7. Chemicals

All chemicals were obtained from Sigma (St. Louis, MO) unless otherwise indicated. Pharmaceutical grade metformin and pioglitazone were a kind gift from regional manufacturers (Pharo Pharma and Hikma Pharmaceuticals).

2.8. Statistical analysis

Values were expressed as mean ± standard error of the mean (SEM). Statistical analysis was done using GraphPad Prism software version 7. Statistical analysis across groups was done using Student's t-test, one-way ANOVA followed by Tukey's post hoc test, and two-way ANOVA followed by Sidak's post hoc test as indicated in the figure legends. P value < 0.05 was considered statistically significant. In CCh concentration–response curves, statistics were run comparing the control

vasodilation and that after different treatment conditions, even though the data might be presented on more than one graph for clarity.

3. Results

3.1. Metabolic consequences of mild hypercaloric feeding

A detailed metabolic and hemodynamic profiling was previously undertaken for this rat model [17–20]. In this study, key phenotypic parameters were confirmed in the rat cohorts used. As expected, there has been no change in body weight, fasting blood glucose, or systolic blood pressure (Fig. 1A–C). On the other hand, fat:lean ratio was increased after twelve weeks of HC feeding (Fig. 1D) indicative of adipose expansion. As well, HC rats showed early signs of metabolic impairment including elevated serum insulin (Fig. 1E) and triglyceride levels (Fig. 1F) confirming the previously reported metabolic consequences. Significantly, twelve weeks of HC diet feeding were associated with renal functional consequences. HC-fed rats had a higher urinary protein concentration (Fig. 1G) and an elevated glomerular filtration rate as measured by the creatinine clearance test (Fig. 1H).

3.2. Alteration in renovascular function following HC feeding in rats:

Fig. 2 depicts several aspects of renovascular endothelial function alteration observed in isolated perfused kidneys from HC-fed rats. Renal perfusion pressure was measured in response to a constant flow rate of 5 ml/min. The average basal renal perfusion pressure amounted to ∼ 75 mmHg in organs isolated from control and HC rats. As expected, an abrupt increase in perfusion pressure occurred upon either increasing the flow rate to 7.5 ml/min or infusing PE at a concentration of 10 µM. Isolated perfused kidneys from HC-fed rats responded by a larger increase in perfusion pressure in response to increased flow (Fig. 2A) or PE infusion (Fig. 2B) indicative of a reduced renal endothelial feedback. To further assess the endothelium-dependent vasodilatory function, the isolated perfused kidneys preconstricted with PE were challenged with a series of CCh concentrations. As shown in the representative tracings (Fig. 2C), HC-fed rat kidneys remained responsive to CCh. However, the observed CCh-evoked dilations in HC-fed rats were not mediated by neither nitric oxide (NO) nor prostaglandins, the typical renovascular endothelial mediators [33], apparent as a lack of an inhibitory effect of a combination of the endothelial nitric oxide synthase (eNOS) inhibitor, LNAME, and the cyclooxygenase inhibitor, diclofenac (Fig. 2E) as seen in isolated perfused kidneys from control rats (Fig. 2D). This was further corroborated by a reduced eNOS phosphorylation at the Akt phosphorylation site in renal cortices from HC rat (Fig. 2F) consistent with a state of vascular insulin resistance. In our previous work [28], drug induced renal dysfunction was associated with upregulation of EET-mediated vasodilation in renal cortices. Indeed, this was the case in HC-fed rats where the EET-mediated component of endothelium-mediated dilation was much enhanced in HC-fed rat kidneys as evident by a much larger change in the CCh response after perfusing the CYP2C inhibitor, MSPPOH (Fig. 2H), compared to control rat tissues (Fig. 2G). Moreover, treatment of control tissues with the 20-HETE synthesis inhibitor, HET0016, led to the expected vasodilation with a consistent reduction of the perfusion pressure by ∼ 10 mmHg at all CCh doses. However, blockade of CYP4A in isolated perfused kidneys from prediabetic rats did not produce a change in perfusion pressure.

3.3. Manifestations of PRAT inflammation in HC-fed rats and amelioration by Met or Pio treatment:

Similar to our previous findings in perivascular adipose inflammation [17], HC feeding was associated with increased UCP-1 expression in PRAT (Fig. 3A). This was also associated with increased adipocyte size seen in H&E-stained PRAT sections (Fig. 3B), increased hypoxia manifesting as elevated HIF1-α expression, no change in CYP2C expression was detected, elevated oxidative stress shown as higher DHE staining, and PRAT inflammation detected by heightened levels of IL-1β compared to PRAT from control rats. Interestingly, two-week treatment with non-hypoglycemic doses of Met or Pio, shown previously to reduce
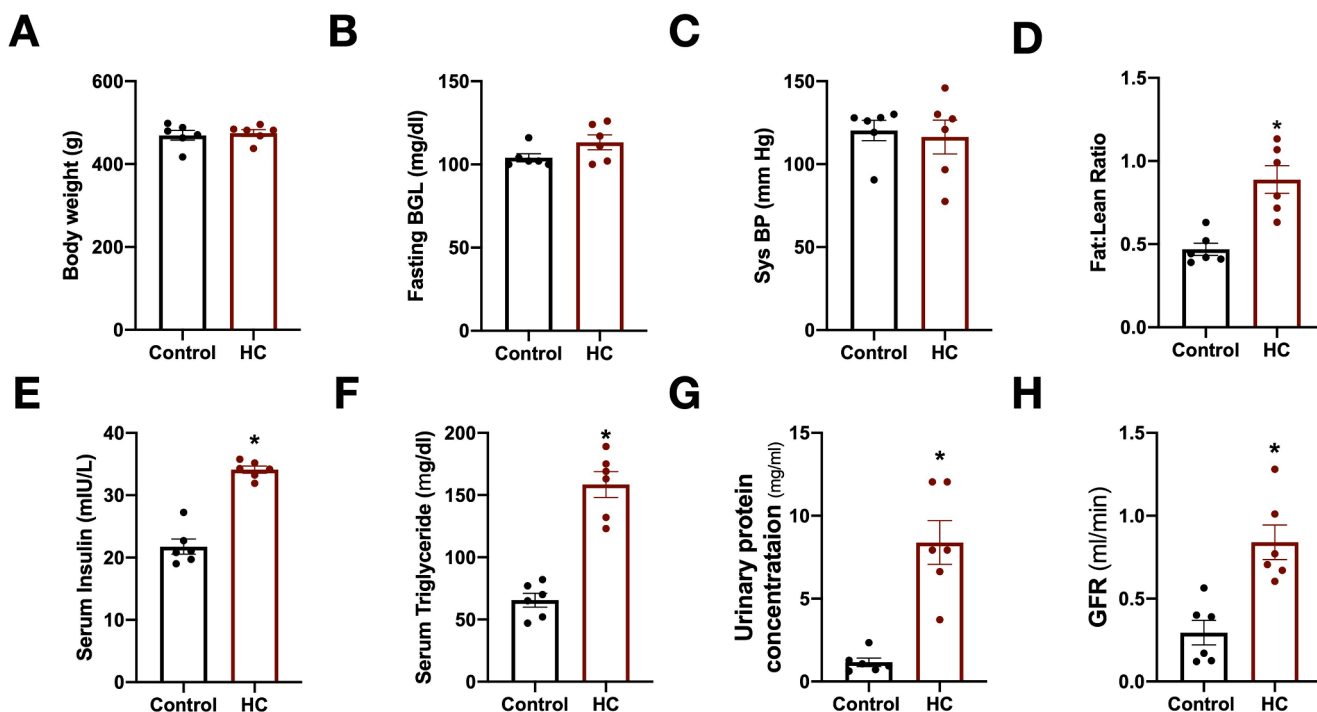

Fig. 1. Metabolic and renal functional characteristic of HC-fed rats. Twelve weeks of HC diet feeding induce a non-obese prediabetic phenotype in rats without an increase in body weight (A), fasting blood glucose (BGL, B), and systolic blood pressure (C); but with increased fat:lean ratio (D), fasting serum insulin (E), and serum triglycerides (F). Renal impairment in these rats manifested as an increased urinary protein (G) and glomerular filtration rate (GFR, H). Results shown are mean ± SEM of observations from six different rats per group. Statistical significance was tested by unpaired Student's *t*-test. * denotes a *P*-value < 0.05.
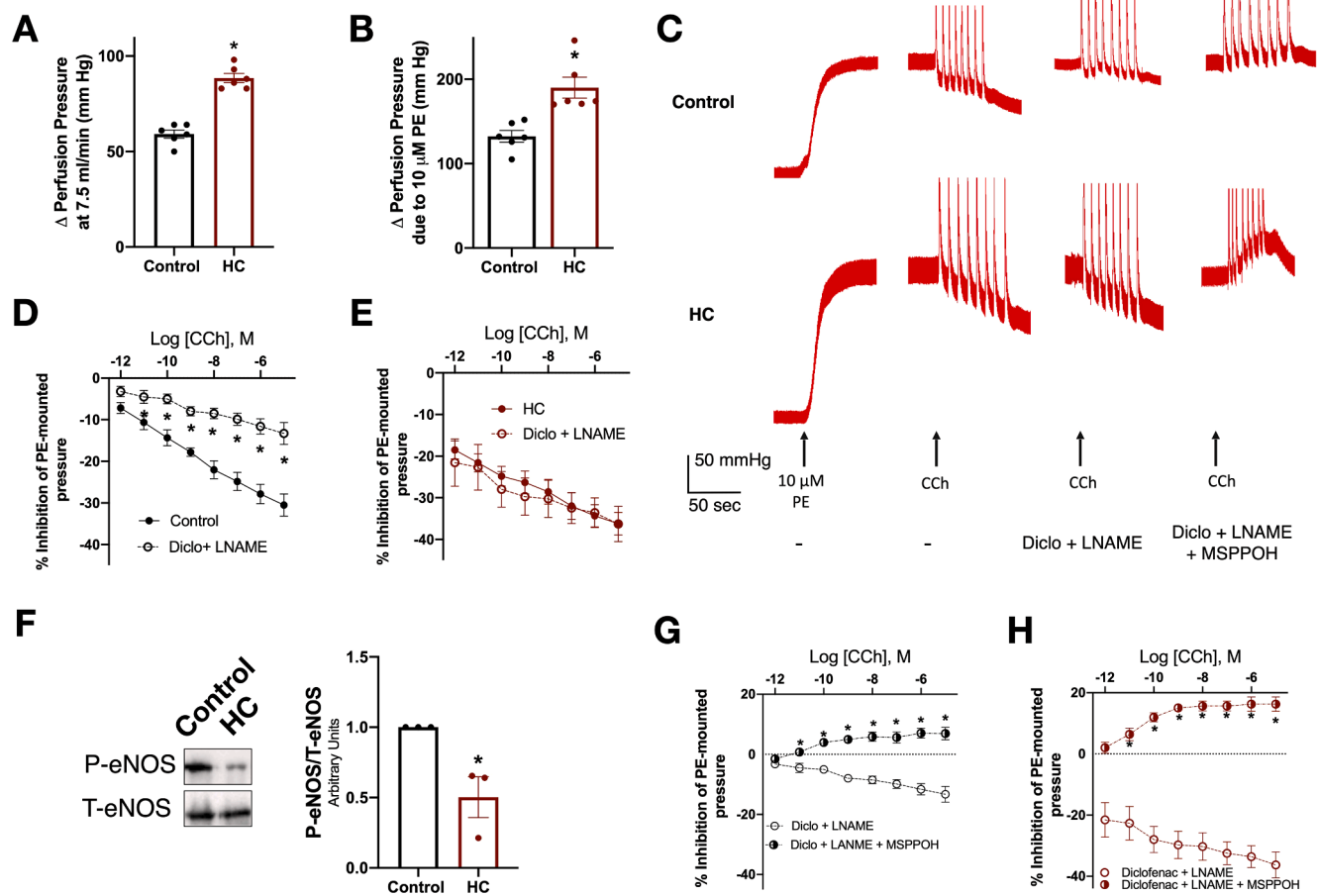
Fig. 2. Renovascular endothelial dysfunction shown in isolated perfused kidneys from control and HC-fed rats. A & B, Reduced endothelial feedback manifested as a larger increase in kidney perfusion pressure in response to increased flow rate or infusion of 10 μM PE, respectively; C, Representative tracings of the CCh-evoked endothelium dependent vasodilation in control (top) and HC-fed rat (bottom) isolated perfused kidneys preconstructed with 10 μM PE in the absence and presence of different inhibitors of prostaglandins, NO, and EET synthesis; D, Summary of CCh-evoked vasodilation in isolated perfused kidneys from control rats in the absence and presence of LNAME/Diclofenac; E, Summary of CCh-evoked vasodilation in isolated perfused kidneys from HC-fed rats in the absence and presence of LNAME/Diclofenac; F, Representative western blots showing eNOS phosphorylation in renal cortical tissue from control and HC-fed rats (left) and summary of quantified data (right). Values depicted are representative of experiments on tissues from three different rats in each group; G, Summary of CCh-evoked vasodilation in isolated perfused kidneys from control (left) and HC-fed (right) rats in presence of LNAME/Diclofenac with or without the CYP2C inhibitor, MSPPOH. Results shown are mean ± SEM of observations from six different rats per group. Statistical significance was tested by unpaired Student's *t*-test for A, B & F and two-way ANOVA followed by Sidak's multiple comparisons test for D, E & G. * denotes a *P*-value < 0.05.

perivascular adipose inflammation [17,19], reversed all of the previous manifestations of PRAT inflammation in HC-fed rats. Significantly, this occurred without an effect on body weight, fat:lean ratio, or serum triglyceride (Fig. 3C). Only Pio treatment reduced PRAT adipocyte size (Fig. 3B) possibly consistent with its ability to reduce serum insulin to values not different from control, though the reduction did not appear to occur robustly across all rats in the treatment group (Fig. 3C).

3.4. HC feeding induces renal cortical inflammatory and structural alterations reversed by Met or Pio treatment:

In parallel to PRAT inflammatory changes, renal cortical tissues from HC-fed rats showed increased expression of inflammatory cytokines including IL-1β, TGF-β1 and VEGF (Fig. 4A and B). While there was no change in renal cortical CYP2C expression, this increase in the pro-inflammatory markers was associated with elevated DHE staining indicative of increased oxidative stress and glomerular sclerosis appearing in the Masson trichrome-stained cortical sections (Fig. 4C). Despite the upregulated expression of TGF-β1, there has been no change in the glomerular mesangial matrix in response to HC feeding. Yet, modest increases and decreases in α-SMA and cytokeratin staining were observed, respectively, (Fig. 4C) possibly consistent with tubular

epithelial-to-mesenchymal *trans*-differentiation (EMT) [34]. Amelioration of PRAT inflammation with the two-week treatment with Met or Pio was associated not only with reduced signs of cortical inflammation, oxidative stress, and structural damage (Fig. 4A–D), but also with the restoration of eNOS phosphorylation levels (Fig. 4A).

3.5. Amelioration of PRAT inflammation restores normal renal functional parameters:

Alongside the positive impact on renal inflammatory and structural alterations, two-week treatment of HC-fed rats with either Met of Pio improved the renal functional deterioration observed in HC-fed rats. Urinary protein levels were reduced (Fig. 5A), together with the elevated glomerular filtration rates (Fig. 5B). Importantly, endothelial feedback in response to both an increased flow rate (Fig. 5C) and PE perfusion (Fig. 5D) was restored to levels that are not different from those seen in isolated perfused kidneys from control rats.

3.6. Treatment with Met or Pio normalized the renal endothelium-mediated vasodilation:

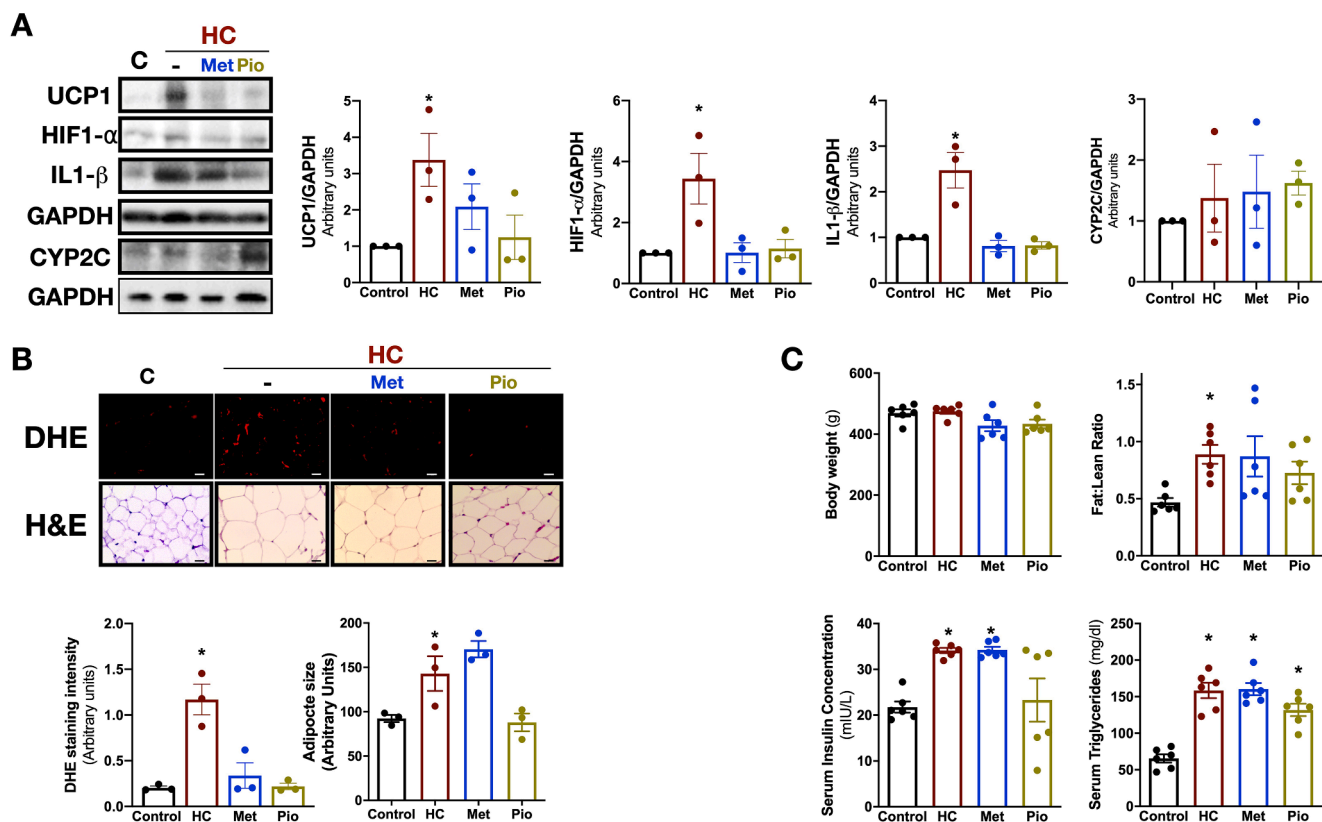Consistent with the observed amelioration of PRAT inflammation

Fig. 3. Manifestations of PRAT inflammation in HC-fed rat and the ameliorative effect of Met and Pio in the absence of an effect on metabolic parameters. A, Representative western blotting (left) and summary of the quantified data (right) showing the expression levels of UCP1, HIF1-α, IL-1β, and CYP2C in PRAT of control, HC-fed and Met- or Pio-treated HC-fed rats; B, Representative micrographs (left) and summary of the quantified data (right) showing the oxidative load in PRAT cryosections as red DHE staining on a black background and adipocyte size in H&E-stained PRAT sections of control. Scale bars are 50 μm for the DHE staining and 25 μm for the H&E staining and Met- or Pio-treated HC-fed rats; C, Two-weeks of Met or Pio treatment neither reduced body weight (top left), fat: lean ratio (top right), nor serum triglyceride (bottom right), with a potential reduction of serum insulin levels in the Pio-treated group to values not significantly different from the control (bottom left). Results shown are mean ± SEM. The blots shown are representatives of experiments on tissues from three different sets of rats, while summary data for micrographs are obtained from nine sections from three different rats per group. For C, observations were obtained from six different rats per group. Statistical significance was tested by one-way ANOVA followed by Tukey multiple comparisons test. * denotes a *P*-value < 0.05 vs. control rat values. (For interpretation of the references to colour in this figure legend, the reader is referred to the web version of this article.)

and renal inflammatory, structural and functional alterations, a two-week treatment with Met or Pio normalized the balance of endothelium-dependent vasodilating mediators. Representative tracings in Fig. 6A show that the sensitivity of the CCh-evoked dilations to LNAME/Diclofenac was restored, with a significant reduction of the dilations after the mixture was perfused (Fig. 6B). Moreover, the EET-dependent vasodilation was reduced as shown by the effect of the CYP2C inhibitor, MSPPOH, on the CCH-induced dilations in isolated perfused kidneys from Met- or Pio-treated HC-fed rats (Fig. 6C). Fig. 6D highlights the increase in the EET-mediated dilatory component in isolated perfused kidneys from HC-fed rats compared to that in organs from control or Met/Pio-treated animals.

3.7. Metabolic and renal consequences following short duration HC feeding

To preclude the possibility that the renal manifestations are a direct effect of HC feeding, an additional group of rats fed HC diet for a shorter period of 4 weeks was examined. As expected, the 4 weeks of HC feeding did not induce any change in body weight, fasting blood glucose, systolic blood pressure, serum insulin or fat:lean ratio (Fig. 7A). Moreover, no change was detected in the urinary protein concentration following 4 weeks of HC feeding. To further asses possible alterations in renovascular endothelial function, kidneys from 4 weeks HC-fed rats were isolated and perfused. As depicted in tracings (Fig. 7B) renal perfusion

pressure was measured in response to PE infusion and CCh-induced dilations were also assessed. No changes in renal endothelial feedback was observed in HC-fed rat kidneys. Moreover, following 4 weeks of HC feeding CCh-evoked dilations were still mediated by NO and prostaglandins same as the control group. This was also confirmed by the consistent eNOS phosphorylation in renal cortices from HC rats following 4 weeks of feeding (Fig. 7C). On the other hand, no changes were seen neither in the inflammatory cytokine IL-1β nor in VEGF expression in renal cortices isolated from 4 weeks HC fed rats (Fig. 7C).

4. Discussion

Recent estimates put diabetic nephropathy at the forefront of causes of CKD-related mortality and morbidity [35]. While tight glycemic control is typically recommended to control diabetic renal involvement, it is not only difficult to achieve, but rather ineffective in improving the prognosis of cardiovascular complications [11,36]. In the present study, we examined the role of PRAT inflammation as an alternative pathological pathway, triggered in early metabolic dysfunction prior to the development of hyperglycemia, which might underlie renal impairment. We show that PRAT inflammation, occurring as an early consequence of metabolic imbalances induced by caloric excess, potentially evokes renal structural and functional deterioration associated with altered renovascular endothelial function. Alteration of endothelium-dependent vasodilator profile and impaired endothelial feedback might underlie
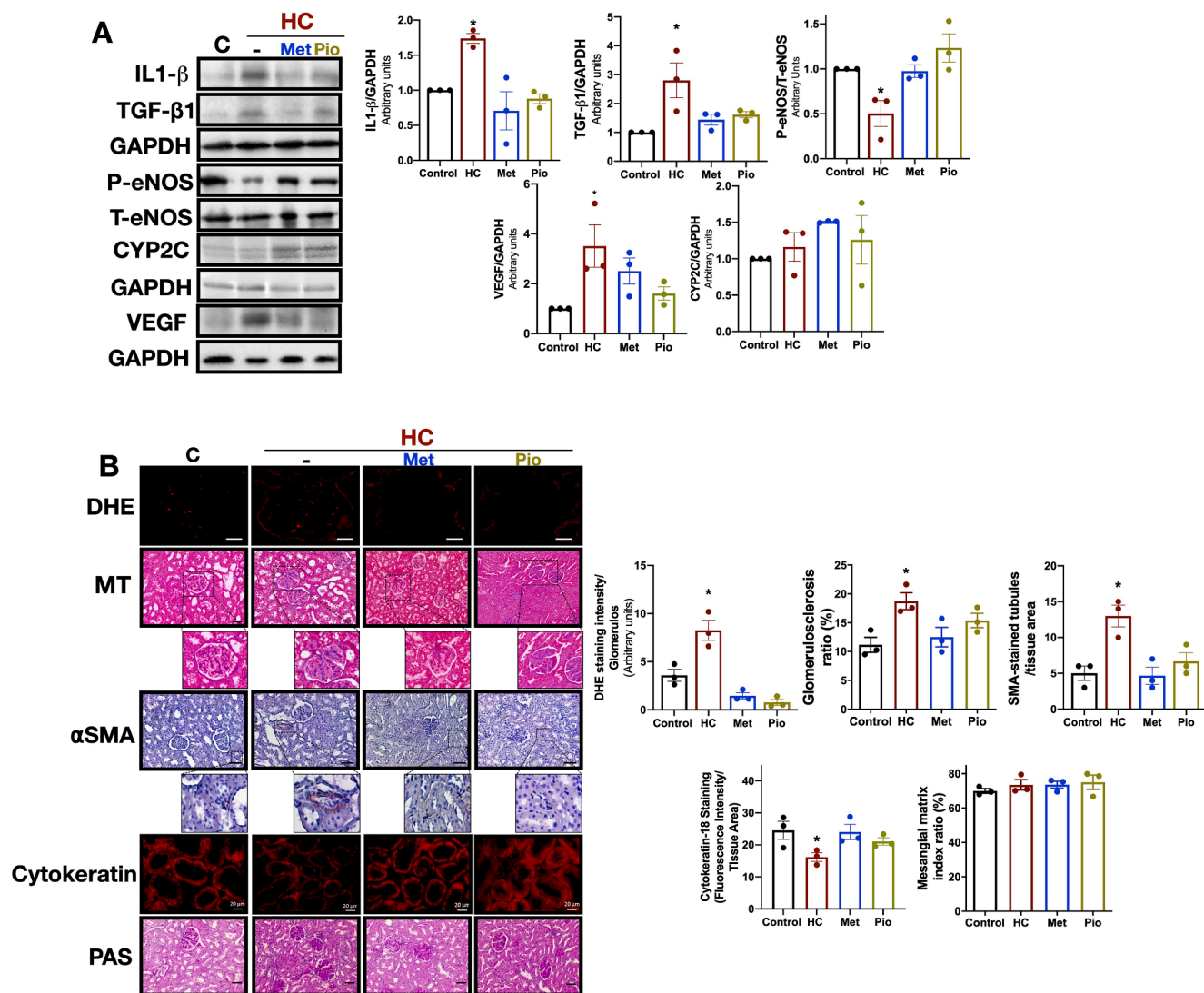
Fig. 4. Signs of molecular and histopathological deterioration in renal cortices of HC-fed rats and their reversal by Met or Pio treatment. Representative western blotting (A) and summary of the quantified data (B) showing the expression levels of IL-1β, TGF-β1, VEGF, CYP2C as well as the phosphorylation levels of eNOS in renal cortices of control, HC-fed and Met- or Pio-treated HC-fed rats, together with representative micrographs (C) and summary of the quantified data (D) showing the glomerular oxidative load in cortical cryosections as red DHE staining on a black background, glomerular fibrotic tissue as blue staining on a red background in Mason's trichrome-stained sections, α-SMA expression as brown staining, cytokeratin expression as red fluorescence on a black background, and mesangial matrix on PAS-stained section from control, HC-fed and Met- or Pio-treated HC-fed rats. Insets in (C) emphasizes areas of interest with representative differences. The scale bars in (C) are 25 µm for DHE staining, 20 µm for cytokeratin staining, and 50 µm for the rest of the micrographs. Results shown are mean ± SEM. The blots shown are representatives of experiments on tissues from three different sets of rats, while summary data for micrographs are obtained from nine sections from three different rats per group. Statistical significance was tested by one-way ANOVA followed by Tukey multiple comparisons test. * denotes a P-value < 0.05 vs. control rat values. (For interpretation of the references to colour in this figure legend, the reader is referred to the web version of this article.)

the observed hyperfiltration and proteinuria. Amelioration of PRAT inflammation at this early stage reversed the observed changes.

For this purpose, we used a rat model of mild metabolic challenge developed in our laboratory, where a limited increase in daily caloric intake from saturated fats and refined sugars leads to a non-obese, hyperinsulinemic prediabetic state following twelve weeks of feeding [17–21]. Indeed, the salient features of this model were confirmed in the cohort of HC-fed rats used in the present study. Particularly, an increased fat:lean ratio was observed in these rats indicative of adipose tissue expansion and potential inflammation. While our previous work consistently showed that this state was associated with neither systemic nor disseminated white adipose depot inflammation [17,19,21], these rats had localized perivascular adipose tissue inflammation. This early involvement of perivascular adipose tissue was attributed to both an increased UCP1 expression together with adipocyte hypertrophy;

concomitant processes occurring due to the peculiar nature of this adipose depot [17]. Here, we show for the first time that a similar localized inflammatory state occurred in PRAT at this early stage of metabolic dysfunction. While studies of the PRAT protein expression profile are scarce, the available evidence shows several levels of UCP1 expression in PRAT adipocytes, which variably correlate with different disease states [37–39]. Similar to perivascular adipose, PRAT in HC-fed rats showed an increased UCP1 expression together with adipocyte hypertrophy. UCP1 increases mitochondrial energy dissipation as heat in a process known as non-shivering thermogenesis that is associated with increased oxygen consumption [40–42]. Such increased demand for oxygen will be augmented by adipocyte hypertrophy triggering PRAT hypoxia. This was indeed the case manifested not only by an increased expression of HIF1-α in HC-fed rat PRAT, but also by a concomitant increase in PRAT reactive oxygen species, an observation commonly encountered with
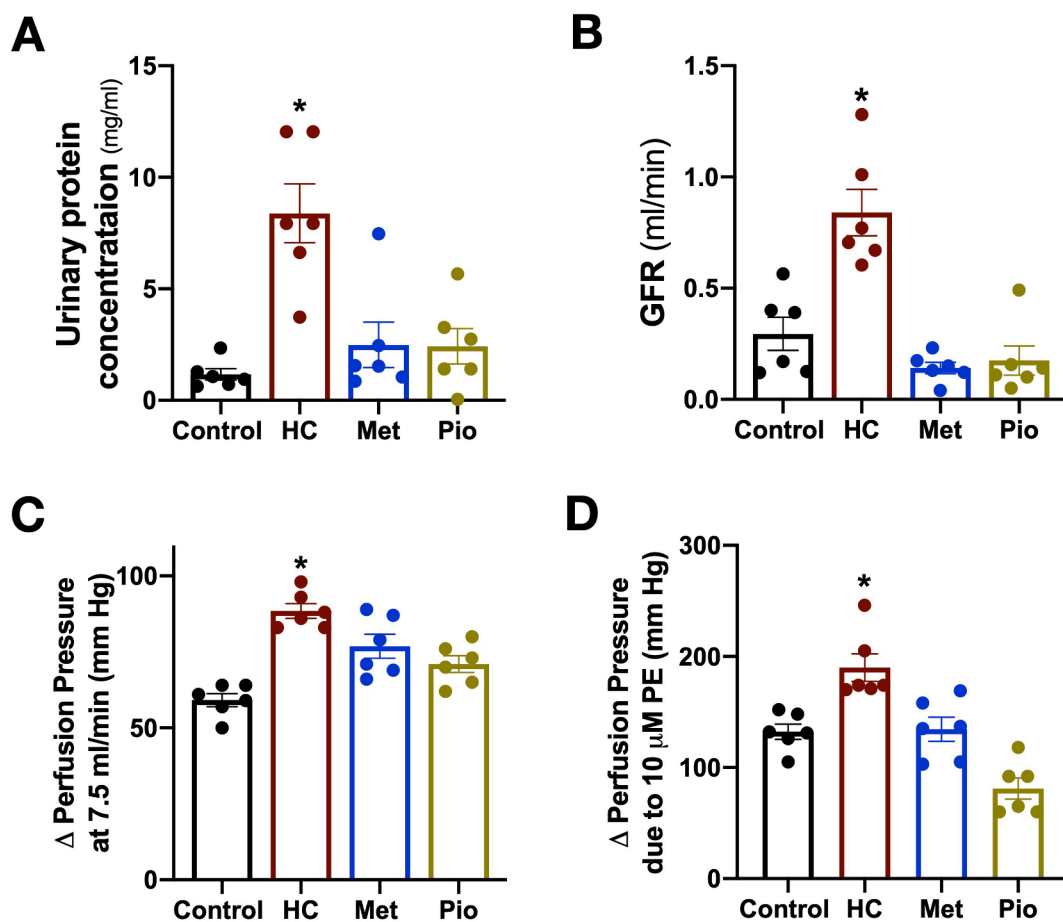
Fig. 5. Amelioration of renal functional manifestations and reduced endothelial feedback in HC-fed rats treated by Met or Pio. The effect of a two-week treatment of HC-fed rats by Met or Pio on urinary protein (A), glomerular filtration rate (B), and the reduced endothelial feedback manifested as an increase in kidney perfusion pressure in response to increased flow rate (C) or infusion of 10 μM PE (D). Results shown are mean ± SEM of observations from six different rats per group. Statistical significance was tested by one-way ANOVA followed by Tukey multiple comparisons test. * denotes a *P*-value < 0.05 vs. control rat values.

adipose expansion in obesity [43]. Hypoxia is a major trigger of adipose tissue inflammation where it activates the NF-κB pathway [44] triggering inflammatory cytokine production, including IL-1β [45,46] as observed in the current results in PRAT isolated from HC-fed rats. Interestingly, altered UCP1 expression and increased PRAT adipocyte size was observed in hypertensive patients [37]. Several mechanisms were proposed for the increased UCP1 expression in metabolic dysfunction including insulin resistance and increased sympathetic stimulation [47], both of which were observed in this prediabetic rat model [17,19,21].

From a renal functional perspective, HC-fed rats showed hyperfiltration and proteinuria. Prior clinical observations suggested that hyperfiltration is a common upstream mechanism that occurs early and drives CKD in type 2 diabetes [5], where it is hypothesized to be a precursor of intraglomerular hypertension inducing proteinuria linked to the progression of CKD [5,48]. Indeed, previous research implicated perirenal fat expansion in microalbuminuria, hyperfiltration, and renal arterial endothelial dysfunction in high-fat fed rats and other animal models of obesity [49,50]. Although the mechanism through which PRAT alters renal function remains elusive, literature primarily suggested a role for mechanical compression of the kidney by the expanding adipose tissue, with a possible contribution of local or systemic inflammatory changes [51]. In the present study, we focus on the early stages of metabolic dysfunction prior to overt obesity or type 2 diabetes. Our results indicate an association among PRAT inflammation, renal functional impairment, renovascular endothelial dysfunction, and renal histological alteration. In the absence of signs of gross cardiovascular

pathology and systemic inflammation with a consistent lack of blood pressure elevation, cardiac ejection fraction abnormalities, and serum cytokine and adipokine profile alteration [17,19–21], a paracrine spillage of inflammatory mediators from PRAT to the renal cortex becomes the likely source of the observed renal functional and structural abnormalities.

In this context, IL-1β was implicated in endothelial dysfunction and reduced NO-mediated endothelium-dependent relaxation in the context of metabolic disease [52]. Significantly, whereas the CCh-evoked endothelium-dependent dilation remained intact, the vascular endothelial feedback was reduced in isolated perfused kidneys from HC-fed rats. Typically, the endothelium responds to increased blood flow and depolarizing vasoconstrictor agents by releasing endothelial vasodilators including NO and prostaglandins [53,54]. As such, it would be expected that endothelial dysfunction would cause the perfused renal vasculature to mount a higher pressure in face of increased flow or a vasoconstrictor challenge. This was indeed the case in isolated perfused kidneys from HC-fed rats where the increase in perfusion pressure in face of higher flow rate or upon stimulation by 10 μM PE was higher than that observed in isolated perfused control kidneys. This observation indicates a possible lack of renovascular buffering of systemic hemodynamic fluctuations. This was corroborated by a diminished contribution of NO/prostaglandins to the observed CCh-evoked relaxation in HC-fed rat kidneys. The reduced eNOS activity could be explained either by the observed reduction in Akt-mediated eNOS phosphorylation as a result of insulin resistance [55] or an IL-1β-induced impairment of eNOS activity directly [56] or via increased oxidative stress [52]. The
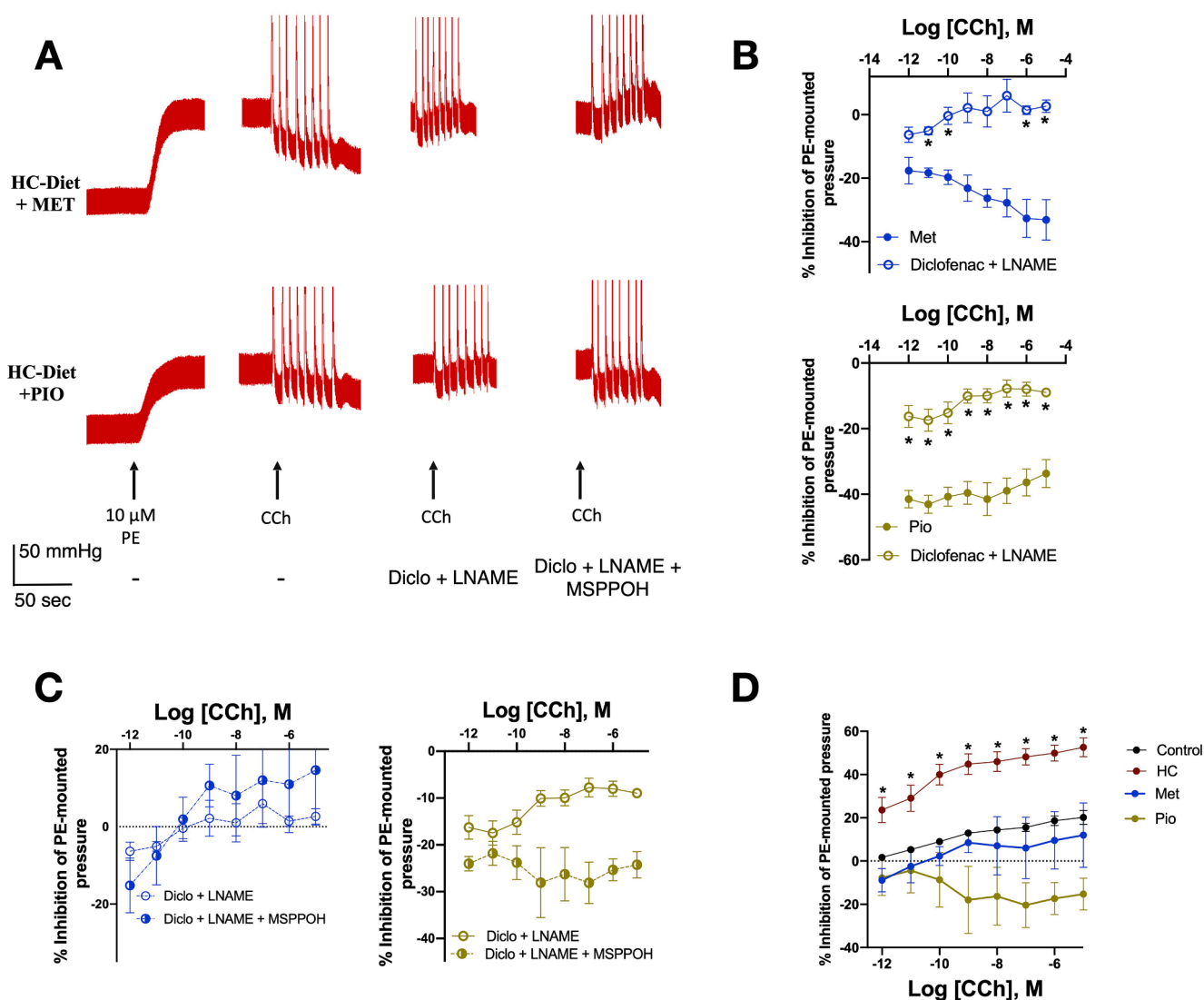
Fig. 6. Normalization of renovascular endothelial function in HC-fed rats following treatment by Met or Pio. A, Representative tracings of the CCh-evoked endothelium dependent vasodilation in Met- (top) and Pio-treated (bottom) HC-fed rat isolated perfused kidneys preconstructed with 10 µM PE in the absence and presence of different inhibitors of prostaglandins, NO, and EET synthesis; B, Summary of CCh-evoked vasodilation in isolated perfused kidneys from Met- (top) and Pio-treated (bottom) HC-fed rats in the absence and presence of LNAME/Diclofenac; C, Summary of CCh-evoked vasodilation in isolated perfused kidneys from Met- (left) and Pio-treated (right) HC-fed rats in the presence of LNAME/Diclofenac with or without the CYP2C inhibitor, MSPPOH; D, Summary of the EET-dependent component of vasodilation at different CCh concentrations in different rat groups. Results shown are mean ± SEM of observations from six different rats per group. Statistical significance was tested by two-way ANOVA followed by Sidak's multiple comparisons test. * denotes a *P*-value < 0.05 vs. the corresponding control.

absence of endothelial feedback was similar to our findings in other vascular beds in the same rat model [18,20]. Significantly, decreased NO availability are known to trigger a detrimental impact of vascular endothelial growth factor (VEGF) on vascular function [57]. Indeed, the reduced glomerular eNOS phosphorylation and NO production observed in obese rats were associated with increased glomerular production of VEGF [58]. In turn, the latter is known to trigger renal endothelial proliferation and increased microvascular permeability potentially underlying the observed proteinuria [59]. Significantly, this was the case in the present study where the reduced eNOS phosphorylation and decreased NO-mediated endothelial vasodilation were associated with increased VEGF expression and proteinuria. Moreover, the augmentation of the EET-mediated component of vasodilation might further contribute to the observed renal functional abnormalities. Importantly, CYP2C-mediated increased EETs production, and an exaggeration of their renovascular dilator effect was previously observed in drug-induced renal inflammatory conditions [28] and was associated with increased renal oxidative stress and inflammatory cytokine production

[32]. Of particular interest, literature describes an intricate balance between endothelial NO and EETs whereby the vasodilatory role of EETs is elicited after NO availability is reduced [60]. In this regards, evidence shows that NO inhibits the catalytic activity of CYP2C without an effect on its protein expression levels [61]. This appears to be the case in our model since western blotting showed that CYP2C expression was not changed in renal cortex in prediabetic rats. Such an adaptive change might reflect the early nature of the kidney injury at this initial stage of metabolic impairment. Significantly, recent literature shows that this endothelial mechanism is lost as patients progress to type 2 diabetes owing to the increased activity of soluble epoxide hydrolase reducing the availability of EETs and attenuating the endothelial vasodilatory response [62]. Given the interaction between cortical NO production and CYP2C activity, it can only be inferred that changes in EET-dependent effects seen in our model are mainly related to CYP2C expression in the renal cortex rather than PRAT, which was dissected off the kidney tissue to allow adequate perfusion. Indeed, CYP2 and the resultant EETs have been shown to reduce adipose tissue inflammation
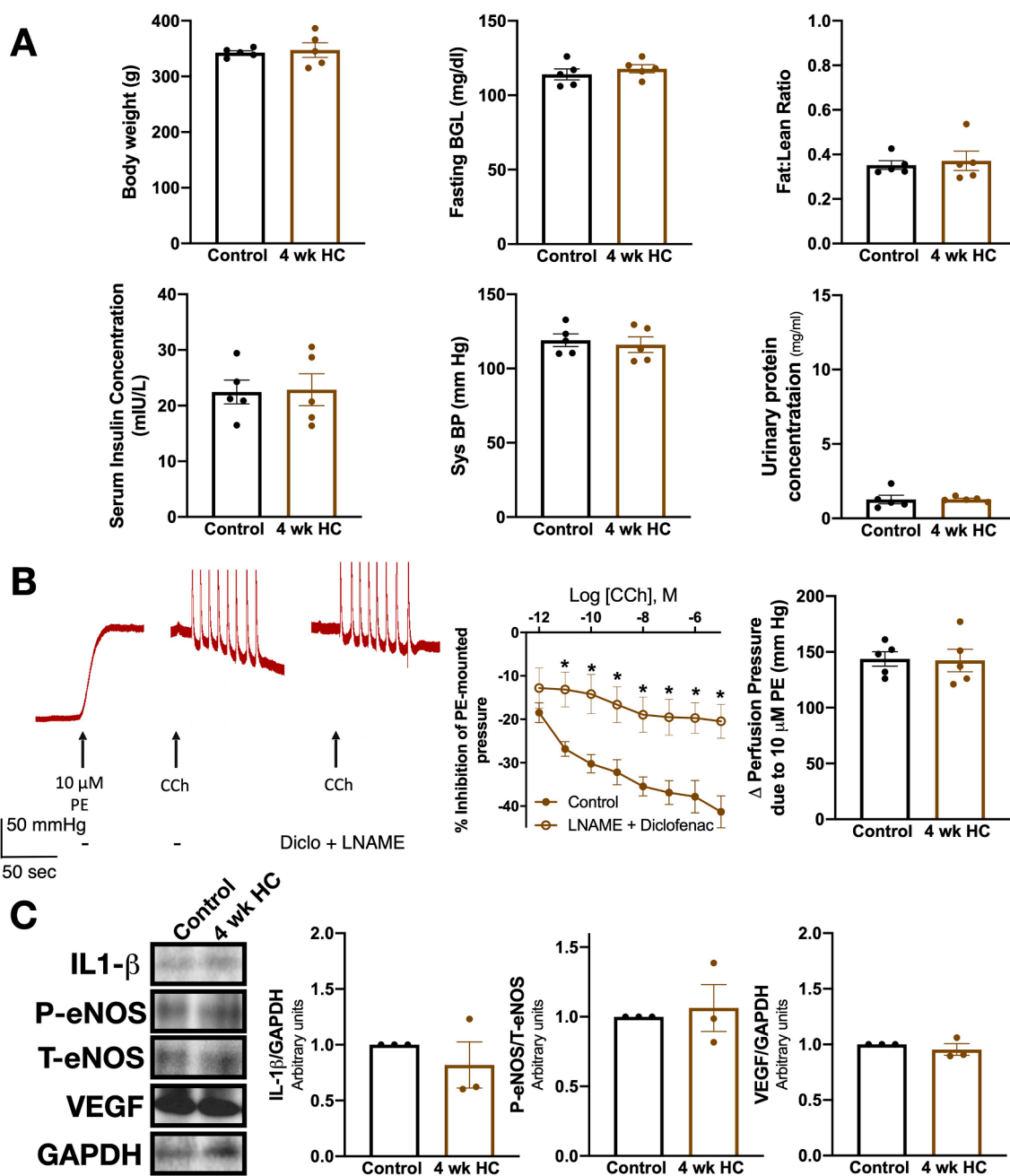
Fig. 7. Metabolic and renovascular endothelial function following 4 weeks of HC feeding. A, Four weeks of HC diet did not induce any change in the metabolic phenotype in rats including body weight, fasting blood glucose (BGL), systolic blood pressure, fasting serum insulin, urinary protein and fat:lean ratio; B, Representative tracings of the CCh-evoked endothelium dependent vasodilation in 4 weeks HC-fed rat isolated perfused kidneys preconstricted with 10 μM PE in the absence and presence of inhibitors of prostaglandins and NO (left), A summary of CCh-evoked vasodilation in isolated perfused kidneys from 4 weeks HC fed rats in the absence and presence of LNAME/Diclofenac appears in the middle, and endothelial feedback in response to infusion of 10 μM PE appears to the right. Results shown are mean ± SEM of observations from five different rats per group compared to their age matched controls; C, Representative western blots showing eNOS phosphorylation, IL-1β, and VEGF in renal cortical tissue from control and 4 weeks HC-fed rats (left) and summary of quantified data (right). The blots shown are representatives of experiments on tissues from three different sets of rats. Statistical significance was tested by unpaired Student's *t*-test. * denotes a *P*-value < 0.05.

and insulin resistance [63], however, their role in PRAT in our model requires further clarification since there was no detectable change in CYP2C expression in PRAT. In further confirmation of the early nature of renal injury, 20-HETE, another arachidonic acid product shown to be involved in hyperglycemia-induced renal damage in later stages of metabolic dysfunction [64], had no role in our present observations in prediabetes. Interestingly, similar to VEGF, EETs have been shown to *trans*-activate growth factor receptors inducing endothelial cell proliferation [65] as well as increase endothelial cell permeability in pathological conditions associated with vascular injury [66]. While this could

potentially imply a role for the observed EETs upregulation in the structural damage observed, it remains far from being ascertained.

Structurally, HC-fed rat renal cortices showed several signs of histopathological and inflammatory changes. Interestingly, IL-1β was shown to induce considerable renal tubular cell damage involving increased production of the profibrogenic cytokine, TGF-β1 [67]. Indeed, increased expression of both IL-1β and TGF-β1 was observed in HC-fed rat renal cortices, together with an elevated glomerular oxidative load, glomerulosclerosis, and possible tubular EMT. However, no increase in mesangial matrix expansion was detected suggesting an early

stage of renal damage in this rat model given that increased mesangial matrix deposition is a hall-mark of kidney injury in advanced stages of metabolic impairment associated with diabetes [68]. We and others previously reported that increased ROS production evokes downstream TGF-β1 expression in renal tissue favoring glomerular fibrosis [32,69]. TGF-β1 enhances extracellular matrix protein deposition in the glomerulus, which in turn causes glomerulosclerosis [48]. Moreover, increased IL-1β/TGF-β1 signaling was shown to underlie increased α-SMA expression and EMT in renal tubular cells leading to renal failure [67,70,71]. Consistent with the proposed early nature of the renal injury, our results showed only modest changes in cytokeratin expression. This is in line with prior studies showing that changes in α-SMA expression occur earlier than changes in cytokeratin expression in response to TGF-β1 [72,73]. Moreover, cytokeratin immunoreactivity persisted *in vivo* in situations where EMT was confirmed with multiple markers such as in severe renal inflammatory conditions, even in tubular epithelial cells expressing α-SMA [74]. Importantly though, the involvement of renal tubular EMT in the context of kidney damage observed in diabetic nephropathy, which we view as the culmination of the pathological process in the current model, is debatable [75,76]. Nevertheless, whether the observed renal structure damage is a direct consequence of a paracrine inflammatory mediator spill from PRAT or a result of exposure to unbuffered hemodynamic stresses evoked by renovascular endothelial dysfunction cannot be directly inferred from our present results. Certainly, both augmented hemodynamic stresses and increased circulating inflammatory mediators were suggested as causes of glomerulopathy, podocyte damage, and proteinuria in advanced obesity [77,78].

To further confirm the role of PRAT inflammation in the observed renal impairment at this early stage of metabolic dysfunction, HC-fed rats were treated by non-hypoglycemic doses of Met or Pio previously shown to mitigate adipose inflammation [79,80]. Such doses consistently demonstrated a reduction in perivascular adipose inflammation in our rat model without an effect on blood glucose level, blood pressure, body weight, or blood lipid levels [17,19,20]. Similar effects were seen in PRAT in the present study. Whereas only Pio reduced serum insulin levels with a consequent reduction of adipocyte size [14], both drugs reduced HIF-1α and IL-1β expression in PRAT of HC-fed rats to control levels. Either drug treatment greatly reduced UCP1 expression offering an explanation for the observed ameliorative effect through reduced oxygen consumption and sensitivity to hypoxia. As well, PRAT oxidative stress was reduced. Reduction of UCP1 expression could possibly be mediated by the insulin sensitizing action of Met and Pio [81,82] and treatment-induced reduction of increased sympathetic activity in this rat model [19,21] and other forms of metabolic dysfunction [83,84]. Amelioration of PRAT inflammation in response to Met or Pio treatment were associated with normalization of the renovascular endothelial function, renal cortex molecular and structural deterioration, hyperfiltration, and proteinuria. Our proposed model of the interaction between early metabolic challenge and PRAT inflammation with the consequent renal dysfunction together with the ameliorative effect of Met and Pio are summarized in Fig. 8. Indeed, the varying effects of Met and Pio observed in some of the cellular and metabolic aspects examined here could be related to peculiarities in the pleiotropic effects of either
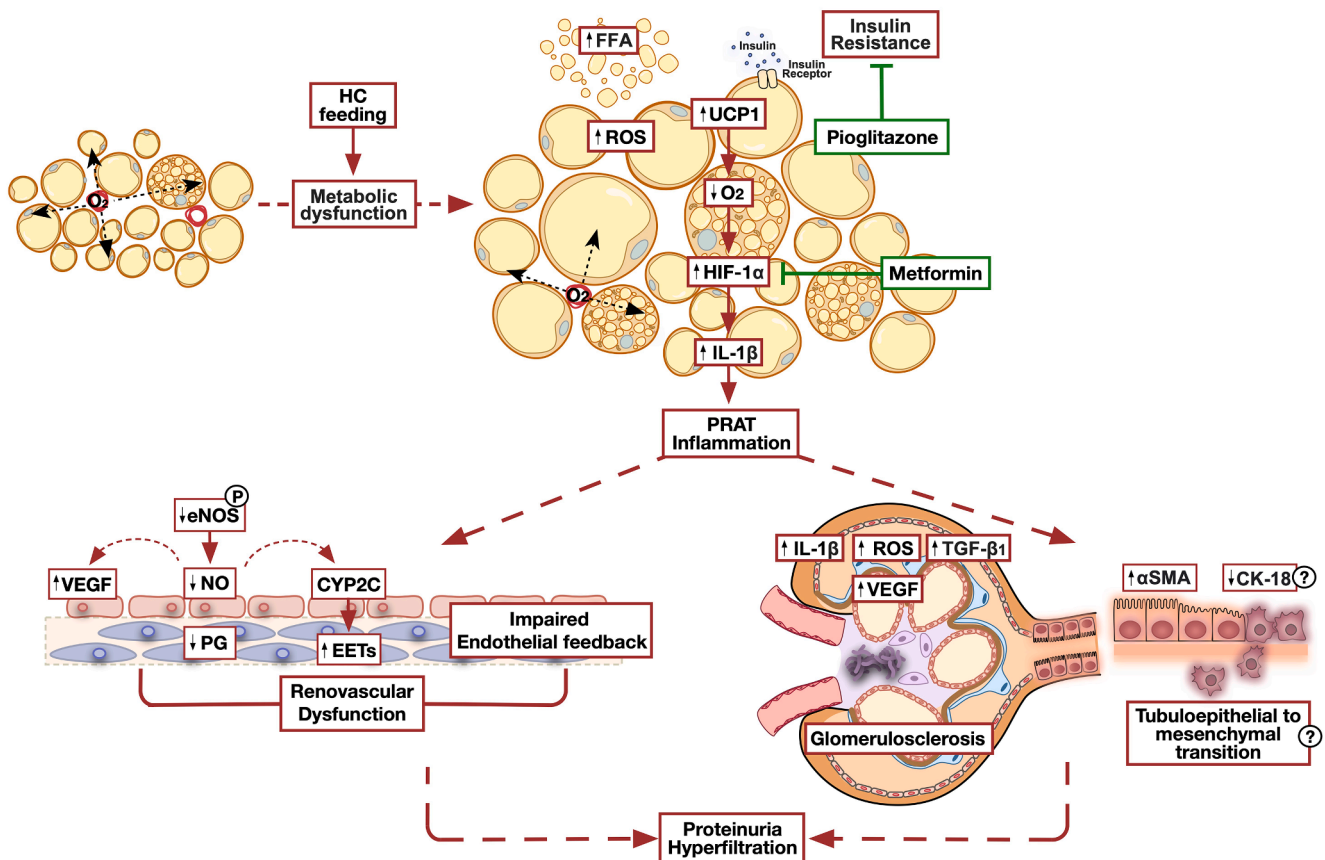

Fig. 8. The proposed model of renal impairment in early metabolic dysfunction transduced by PRAT inflammation. Even mild increases in calorie intake would drive metabolic changes leading to adipose tissue remodeling. PRAT responding both by adipocyte hypertrophy and upregulated UCP1 expression becomes sensitive to hypoxic changes leading to inflammation and increased production of inflammatory cytokines. Paracrine transfer of the produced cytokines trigger renal endothelial and structural deterioration observed as loss of endothelial feedback, increased glomerular sclerosis, increased tubular epithelial-to-mesenchymal *trans*-differentiation, hyperfiltration, and proteinuria. Amelioration of PRAT inflammation by Met and Pio decreases the consequent renal manifestations and normalizes renal function.

drug. For instance, Met is known to switch the cellular metabolism into an anaerobic state [85], and thus would drastically lower the cellular demand for oxygen in adipocytes [86] directly alleviating hypoxia, whereas Pio being a PPARγ agonist might have promoted adipocyte progenitor cell recruitment and hyperplastic rather than hypertrophic PRAT expansion [87,88] associated with reduced adipocyte size, and thus decreased hypoxia.

To further confirm our model and rule out a potential direct effect of exposure to saturated fat and refined sugars in the HC diet, we conducted further experiments in rats exposed only to four weeks of HC diet feeding. While being a considerable duration of exposure, a four-week feeding protocol neither triggered hyperinsulinemia nor adipose expansion that underlie adipose tissue inflammation. Under such circumstances, a normal renovascular endothelial function was observed as well as normal renal cortical levels of eNOS phosphorylation and VEGF and IL-1β expression compared to age-matched controls.

One limitation of the present study is that a direct effect of the *in vivo* treatment with either Met or Pio on renovascular endothelial function that is not mediated by an ameliorative effect on PRAT could not be ruled out. However, studies evaluating the effect of either drug on vascular endothelial function in the context of early metabolic impairment report concomitant improvement of markers of adipose tissue dysfunction [89–91]. Moreover, our present and previous results [17] consistently show that adipose inflammation is the only detrimental consequence of mild metabolic challenge to be reversed by the doses of Met and Pio used suggesting that alternative bystander pathways are rather unlikely.

In conclusion, our present results strongly implicate localized PRAT inflammation as a cause of renal impairment early in the course of metabolic deterioration. The paracrine effects of PRAT inflammatory mediators lead to renovascular endothelial dysfunction, hyperfiltration, renal cortical inflammation and proteinuria. Met and Pio ameliorate PRAT inflammation potentially leading to disease modifying effects correcting the initial pathological pathways resulting in diabetic nephropathy. Even though selective tools targeting TGF- β1 and VEGF implicated as mediators of the detrimental effect seen in this model exits, the available evidence indicate that their complete blockade using monoclonal antibodies might be associated with harm in diabetic nephropathy [92,93] emphasizing the potential value of targeting PRAT inflammation. Future research into tailored pharmacological tools for this purpose is warranted.

CRediT authorship contribution statement

Safaa H. Hammoud: Investigation, Writing - original draft. **Ibrahim Al-Zaim:** Investigation. **Nahed Mougharbil:** Investigation. **Sahar Koubar:** Funding acquisition, Resources, Writing - review & editing. **Ali H. Eid:** Resources, Writing - review & editing. **Assaad A. Eid:** Methodology, Formal analysis, Funding acquisition, Writing - review & editing. **Ahmed F. El-Yazbi:** Conceptualization, Methodology, Formal analysis, Resources, Writing - original draft, Writing - review & editing, Visualization, Supervision, Project administration, Funding acquisition.

Declaration of Competing Interest

The authors declare that they have no known competing financial interests or personal relationships that could have appeared to influence the work reported in this paper.

Acknowledgement

References

[1] WHO, Non communicable diseases country profiles 2018 (2018).

[2] K. Papatheodorou, M. Banach, E. Bekiari, M. Rizzo, M. Edmonds, Complications of Diabetes 2017, J. Diabetes Res. 2018 (2018) 3086167.

[3] J.C. Lv, L.X. Zhang, Prevalence and disease burden of chronic kidney disease, Adv. Exp. Med. Biol. 1165 (2019) 3–15.

[4] P.H. Winocour, Diabetes and chronic kidney disease: an increasingly common multi-morbid disease in need of a paradigm shift in care, Diabet. Med. 35 (3) (2018) 300–305.

[5] H.J. Anders, T.B. Huber, B. Isermann, M. Schiffer, CKD in diabetes: diabetic kidney disease versus nondiabetic kidney disease, Nat. Rev. Nephrol. 14 (6) (2018) 361–377.

[6] A. American Diabetes, 6. Glycemic Targets: Standards of Medical Care in Diabetes-2018, Diabetes Care 41 (Suppl 1) (2018) S55–S64.

[7] E.W. Gregg, Y. Li, J. Wang, N.R. Burrows, M.K. Ali, D. Rolka, D.E. Williams, L. Geiss, Changes in diabetes-related complications in the United States, 1990–2010, N. Engl. J. Med. 370 (16) (2014) 1514–1523.

[8] A. Andres-Hernando, M.A. Lanaspa, M. Kuwabara, D.J. Orlicky, C. Cicerchi, E. Bales, G.E. Garcia, C.A. Roncal-Jimenez, Y. Sato, R.J. Johnson, Obesity causes renal mitochondrial dysfunction and energy imbalance and accelerates chronic kidney disease in mice, Am. J. Physiol. Renal Physiol. 317 (4) (2019) F941–F948.

[9] S.J. Glastras, H. Chen, R. Teh, R.T. McGrath, J. Chen, C.A. Pollock, M.G. Wong, S. Saad, Mouse models of diabetes, obesity and related kidney disease, PLoS One 11 (8) (2016), e0162131.

[10] S.E. Wicks, T.T. Nguyen, C. Breaux, C. Kruger, K. Stadler, Diet-induced obesity and kidney disease – In search of a susceptible mouse model, Biochimie 124 (2016) 65–73.

[11] Y. Barer, O. Cohen, T. Cukierman-Yaffe, Effect of glycaemic control on cardiovascular disease in individuals with type 2 diabetes with pre-existing cardiovascular disease: A systematic review and meta-analysis, Diabetes Obes. Metab. 21 (3) (2019) 732–735.

[12] D.H. Wasserman, T.J. Wang, N.J. Brown, The vasculature in prediabetes, Circ. Res. 122 (8) (2018) 1135–1150.

[13] A. Festa, A.J. Hanley, R.P. Tracy, R. D'Agostino Jr., S.M. Haffner, Inflammation in the prediabetic state is related to increased insulin resistance rather than decreased insulin secretion, Circulation 108 (15) (2003) 1822–1830.

[14] D.J. Pedersen, A. Guilherme, L.V. Danai, L. Heyda, A. Matevossian, J. Cohen, S. M. Nicoloro, J. Straubhaar, H.L. Noh, D. Jung, J.K. Kim, M.P. Czech, A major role of insulin in promoting obesity-associated adipose tissue inflammation, Mol. Metab. 4 (7) (2015) 507–518.

[15] H. Xu, G.T. Barnes, Q. Yang, G. Tan, D. Yang, C.J. Chou, J. Sole, A. Nichols, J. S. Ross, L.A. Tartaglia, H. Chen, Chronic inflammation in fat plays a crucial role in the development of obesity-related insulin resistance, J. Clin. Invest. 112 (12) (2003) 1821–1830.

[16] A.C. Webster, E.V. Nagler, R.L. Morton, P. Masson, Chronic kidney disease, Lancet 389 (10075) (2017) 1238–1252.

[17] M.A.W. Elkhatib, A. Mroueh, R.W. Rafeh, F. Sleiman, H. Fouad, E.I. Saad, M. A. Fouda, O. Elgaddar, K. Issa, A.H. Eid, A.A. Eid, K.S. Abd-Elrahman, A.F. El-Yazbi, Amelioration of perivascular adipose inflammation reverses vascular dysfunction in a model of nonobese prediabetic metabolic challenge: Potential role of antidiabetic drugs, Transl. Res. 214 (2019) 121–143.

[18] R. Alaaeddine, M.A.W. Elkhatib, A. Mroueh, H. Fouad, E.I. Saad, M.E. El-Sabban, F. Plane, A.F. El-Yazbi, Impaired endothelium-dependent hyperpolarization underlies endothelial dysfunction during early metabolic challenge: Increased ROS Generation and Possible Interference with NO Function, J. Pharmacol. Exp. Ther. 371 (3) (2019) 567–582.

[19] O. Al-Assi, R. Ghali, A. Mroueh, A. Kaplan, N. Mougharbil, A.H. Eid, F.A. Zouein, A. F. El-Yazbi, Cardiac autonomic neuropathy as a result of mild hypercaloric challenge in absence of signs of diabetes: modulation by antidiabetic drugs, Oxid Med. Cell Longev. 2018 (2018) 9389784.

[20] W. Fakih, A. Mroueh, H. Salah, A.H. Eid, M. Obeid, F. Kobeissy, H. Darwish, A. F. El-Yazbi, Dysfunctional cerebrovascular tone contributes to cognitive impairment in a non-obese rat model of prediabetic challenge: Role of suppression of autophagy and modulation by anti-diabetic drugs, Biochem. Pharmacol. 178 (2020), 114041.

[21] N.M.Z. Bakkar, N. Mougharbil, A. Mroueh, A. Kaplan, A.H. Eid, S.A. Fares, F. Zouein, A. El-Yazbi, Worsening Baroreflex Sensitivity on Progression to Type II Diabetes: Localized vs. Systemic Inflammation and Role of Antidiabetic Therapy, American journal of physiology. Endocrinology and metabolism (2020).

[22] M.M. El-Mas, H.M. El-Gowelli, K.S. Abd-Elrahman, E.I. Saad, A.G. Abdel-Galil, A. A. Abdel-Rahman, Pioglitazone abrogates cyclosporine-evoked hypertension via rectifying abnormalities in vascular endothelial function, Biochem. Pharmacol. 81 (4) (2011) 526–533.

[23] N. Apaijai, H. Pintana, S.C. Chattipakorn, N. Chattipakorn, Cardioprotective effects of metformin and vildagliptin in adult rats with insulin resistance induced by a high-fat diet, Endocrinology 153 (8) (2012) 3878–3885.

[24] R.P. Rao, A. Singh, A.K. Jain, B.P. Srinivasan, Dual therapy of rosiglitazone/ pioglitazone with glimepiride on diabetic nephropathy in experimentally induced type 2 diabetes rats, J. Biomed. Res. 25 (6) (2011) 411–417.

[25] O. Al-Assi, R. Ghali, A. Mroueh, A. Kaplan, N. Mougharbil, A.H. Eid, Cardiac autonomic neuropathy as a result of mild hypercaloric challenge in absence of signs of diabetes: Modulation by antidiabetic, Drugs 2018 (2018) 9389784.

[26] Y. Wang, S.E. Thatcher, L.A. Cassis, Measuring blood pressure using a noninvasive tail cuff method in mice, Methods Mol. Biol. 1614 (2017) 69–73.

[27] M. Prakash, J.K. Shetty, S. Dash, B.K. Barik, A. Sarkar, R. Prabhu, Determination of urinary peptides in patients with proteinuria, Indian J. Nephrol. 18 (4) (2008) 150–154.

[28] S.H. Hammoud, A.G. Omar, A.A. Eid, M.M. El-Mas, CYP4A/CYP2C modulation of the interaction of calcium channel blockers with cyclosporine on EDHF-mediated renal vasodilations in rats, Toxicol. Appl. Pharmacol. 334 (2017) 110–119.

[29] N. Miyata, K. Taniguchi, T. Seki, T. Ishimoto, M. Sato-Watanabe, Y. Yasuda, M. Doi, S. Kametani, Y. Tomishima, T. Ueki, M. Sato, K. Kameo, HET0016, a potent and selective inhibitor of 20-HETE synthesizing enzyme, Br. J. Pharmacol. 133 (3) (2001) 325–329.

[30] H. Huang, H.H. Chang, Y. Xu, D.S. Reddy, J. Du, Y. Zhou, Z. Dong, J.R. Falck, M. H. Wang, Epoxyeicosatrienoic Acid inhibition alters renal hemodynamics during pregnancy, Experimental biology and medicine (Maywood, N.J.) 231 (11) (2006) 1744–1752.

[31] P.R. Johnson, J. Hirsch, Cellularity of adipose depots in six strains of genetically obese mice, J. Lipid Res. 13 (1) (1972) 2–11.

[32] S.H. Hammoud, S. Alkhansa, N. Mahjoub, A.G. Omar, M.M. El-Mas, A.A. Eid, Molecular basis of the counteraction by calcium channel blockers of cyclosporine nephrotoxicity, Am. J. Physiol. Renal Physiol. 315 (3) (2018) F572–F582.

[33] N. Jourde-Chiche, F. Fakhouri, L. Dou, J. Bellien, S. Burtey, M. Frimat, P.-A. Jarrot, G. Kaplanski, M. Le Quintrec, V. Pernin, C. Rigothier, M. Sallée, V. Fremeaux-Bacchi, D. Guerrot, L.T. Roumenina, Endothelium structure and function in kidney health and disease, Nat. Rev. Nephrol. 15 (2) (2019) 87–108.

[34] Y.-Y. Ng, T.-P. Huang, W.-C. Yang, Z.-P. Chen, A.-H. Yang, W. Mu, D.J. Nikolic-Paterson, R.C. Atkins, H.Y. Lan, Tubular epithelial-myofibroblast transdifferentiation in progressive tubulointerstitial fibrosis in 5/6 nephrectomized rats, Int. 54 (3) (1998) 864–876.

[35] GBD Chronic Kidney Disease Collaboration, Global, regional, and national burden of chronic kidney disease, 1990–2017: A systematic analysis for the Global Burden of Disease Study 2017, Lancet 395 (10225) (2020) 709–733.

[36] S.J. Griffin, K. Borch-Johnsen, M.J. Davies, K. Khunti, G.E. Rutten, A. Sandbæk, S. J. Sharp, R.K. Simmons, M. van den Donk, N.J. Wareham, T. Lauritzen, Effect of early intensive multifactorial therapy on 5-year cardiovascular outcomes in individuals with type 2 diabetes detected by screening (ADDITION-Europe): A cluster-randomised trial, Lancet 378 (9786) (2011) 156–167.

[37] X. Li, J. Liu, G. Wang, J. Yu, Y. Sheng, C. Wang, Y. Lv, S. Lv, H. Qi, W. Di, C. Yin, G. Ding, Determination of UCP1 expression in subcutaneous and perirenal adipose tissues of patients with hypertension, Endocrine 50 (2) (2015) 413–423.

[38] X. Li, G. Wang, J. Liu, G. Ding, Increased UCP1 expression in the perirenal adipose tissue of patients with renal cell carcinoma, Oncol. Rep. 42 (5) (2019) 1972–1980.

[39] N.Z. Jespersen, A. Feizi, E.S. Andersen, S. Heywood, H.B. Hattel, S. Daugaard, L. Peijs, P. Bagi, B. Feldt-Rasmussen, H.S. Schultz, N.S. Hansen, R. Krogh-Madsen, B.K. Pedersen, N. Petrovic, S. Nielsen, C. Scheele, Heterogeneity in the perirenal region of humans suggests presence of dormant brown adipose tissue that contains brown fat precursor cells, Molec. Metabol. 24 (2019) 30–43.

[40] I.G. Shabalina, N. Petrovic, J.M. de Jong, A.V. Kalinovich, B. Cannon, J. Nedergaard, UCP1 in brite/beige adipose tissue mitochondria is functionally thermogenic, Cell Rep. 5 (5) (2013) 1196–1203.

[41] G.H.E.J. Vijgen, L.M. Sparks, N.D. Bouvy, G. Schaart, J. Hoeks, W.D. van Marken Lichtenbelt, P. Schrauwen, Increased oxygen consumption in human adipose tissue from the "Brown Adipose Tissue" Region, J. Clin. Endocrinol. Metabol. 98 (7) (2013) E1230–E1234.

[42] K. Schneider, J. Valdez, J. Nguyen, M. Vawter, B. Galke, T.W. Kurtz, J.Y. Chan, Increased energy expenditure, Ucp1 expression, and resistance to diet-induced obesity in mice lacking nuclear factor-erythroid-2-related Transcription Factor-2 (Nrf2), J. Biol. Chem. 291 (14) (2016) 7754–7766.

[43] C.Y. Han, Roles of reactive oxygen species on insulin resistance in adipose tissue, Diabetes Metabol. J. 40 (4) (2016) 272–279.

[44] L. D'Ignazio, S. Rocha, Hypoxia Induced NF-κB, Cells 5 (1) (2016) 10.

[45] D.S. Dzhalilova, A.M. Kosyreva, M.E. Diatroptov, E.A. Ponomarenko, I.S. Tsvetkov, N.A. Zolotova, V.A. Mkhitarov, D.N. Khochanskiy, O.V. Makarova, Dependence of the severity of the systemic inflammatory response on resistance to hypoxia in male Wistar rats, J. Inflam. Res. 12 (2019) 73–86.

[46] H.-J. Jeong, S.-H. Hong, R.-K. Park, T. Shin, N.-H. An, H.-M. Kim, Hypoxia-induced IL-6 production is associated with activation of MAP kinase, HIF-1, and NF-κB on HEI-OC1 cells, Hear. Res. 207 (1) (2005) 59–67.

[47] R. Rafeh, A. Viveiros, G.Y. Oudit, A.F. El-Yazbi, Targeting perivascular and epicardial adipose tissue inflammation: therapeutic opportunities for cardiovascular disease, Clinical science (London, England : 1979) 134(7) (2020) 827-851.

[48] P. Palatini, Glomerular hyperfiltration: a marker of early renal damage in pre-diabetes and pre-hypertension, Nephrol. Dial. Transplant. 27 (5) (2012) 1708–1714.

[49] N. Hou, F. Han, M. Wang, N. Huang, J. Zhao, X. Liu, X. Sun, Perirenal fat associated with microalbuminuria in obese rats, Int. Urol. Nephrol. 46 (4) (2014) 839–845.

[50] S. Ma, X.-Y. Zhu, A. Eirin, J.R. Woollard, K.L. Jordan, H. Tang, A. Lerman, L. O. Lerman, Perirenal fat promotes renal arterial endothelial dysfunction in obese swine through tumor necrosis factor-α, J. Urol. 195 (4 Pt 1) (2016) 1152–1159.

[51] N. Huang, E.-W. Mao, N.-N. Hou, Y.-P. Liu, F. Han, X.-D. Sun, Novel insight into perirenal adipose tissue: A neglected adipose depot linking cardiovascular and chronic kidney disease, World J. Diabetes 11 (4) (2020) 115–125.

[52] S. Vallejo, E. Palacios, T. Romacho, L. Villalobos, C. Peiró, C.F. Sánchez-Ferrer, The interleukin-1 receptor antagonist anakinra improves endothelial dysfunction in streptozotocin-induced diabetic rats, Cardiovasc. Diabetol. 13 (1) (2014) 158.

[53] Z. Peng, B. Shu, Y. Zhang, M. Wang, Endothelial response to pathophysiological stress, Arterioscler. Thromb. Vasc. Biol. 39 (11) (2019) e233–e243.

[54] K.A. Dora, J.M. Hinton, S.D. Walker, C.J. Garland, An indirect influence of phenylephrine on the release of endothelium-derived vasodilators in rat small mesenteric artery, Br. J. Pharmacol. 129 (2) (2000) 381–387.

[55] R. Muniyappa, J.R. Sowers, Role of insulin resistance in endothelial dysfunction, Rev. Endocr. Metab. Disord. 14 (1) (2013) 5–12.

[56] Y. Kawasaki, E. Yokobayashi, K. Sakamoto, E. Tenma, H. Takaki, Y. Chiba, T. Otashiro, M. Ishihara, S. Yonezawa, A. Sugiyama, Y. Natori, Angiostatin prevents IL-1β-induced down-regulation of eNOS expression by inhibiting the NF-κB cascade, J. Pharmacol. Sci. 129 (3) (2015) 200–204.

[57] J. Karalliedde, L. Gnudi, Endothelial factors and diabetic nephropathy, Diabetes Care 34 (Supplement 2) (2011) S291.

[58] X. Sun, Y. Yu, L. Han, High FFA levels related to microalbuminuria and uncoupling of VEGF-NO axis in obese rats, Int. Urol. Nephrol. 45 (4) (2013) 1197–1207.

[59] T. Nakagawa, Uncoupling of the VEGF-endothelial nitric oxide axis in diabetic nephropathy: An explanation for the paradoxical effects of VEGF in renal disease, Am.J. Physiol. Renal Physiol. 292 (6) (2007) F1665–F1672.

[60] T. Hillig, P. Krustrup, I. Fleming, T. Osada, B. Saltin, Y. Hellsten, Cytochrome P450 2C9 plays an important role in the regulation of exercise-induced skeletal muscle blood flow and oxygen uptake in humans, J. Physiol. 546 (Pt 1) (2003) 307–314.

[61] E.T. Morgan, C. Skubic, C.M. Lee, K.B. Cokan, D. Rozman, Regulation of cytochrome P450 enzyme activity and expression by nitric oxide in the context of inflammatory disease, Drug Metab. Rev. 52 (4) (2020) 455–471.

[62] T. Duflot, L. Moreau-Grangé, C. Roche, M. Iacob, J. Wils, I. Rémy-Jouet, A.-F. Cailleux, M. Leuillier, S. Renet, D. Li, C. Morisseau, F. Lamoureux, V. Richard, G. Prévost, R. Joannidès, J. Bellien, Altered bioavailability of epoxyeicosatrienoic acids is associated with conduit artery endothelial dysfunction in type 2 diabetic patients, Cardiovasc. Diabetol. 18 (1) (2019) 35.

[63] M. Dai, L. Wu, P. Wang, Z. Wen, X. Xu, D.W. Wang, CYP2J2 and Its Metabolites EETs Attenuate Insulin Resistance via Regulating Macrophage Polarization in Adipose Tissue, Sci. Rep. 7 (1) (2017) 46743.

[64] S. Eid, R. Maalouf, A.A. Jaffa, J. Nassif, A. Hamdy, A. Rashid, F.N. Ziyadeh, A. A. Eid, 20-HETE and EETs in diabetic nephropathy: a novel mechanistic pathway, PLoS One 8 (8) (2013) e70029.

[65] I. Fleming, R. Busse, Endothelium-derived epoxyeicosatrienoic acids and vascular function, Hypertension 47 (4) (2006) 629–633.

[66] D.F. Alvarez, E.A. Gjerde, M.I. Townsley, Role of EETs in regulation of endothelial permeability in rat lung, American journal of physiology, Lung Cell. Mole. Physiol. 286 (2) (2004) L445–L451.

[67] D.A. Vesey, C.W. Cheung, L. Cuttle, Z.A. Endre, G. Gobé, D.W. Johnson, Interleukin-1beta induces human proximal tubule cell injury, alpha-smooth muscle actin expression and fibronectin production, Kidney Int. 62 (1) (2002) 31–40.

[68] T. Wang, Y. Gao, X. Wang, Y. Shi, J. Xu, B. Wu, J. He, Y. Li, Calpain-10 drives podocyte apoptosis and renal injury in diabetic nephropathy, Diabetes Metab. Syndrome Obesity: Targets Therapy 12 (2019) 1811–1820.

[69] S. Akool el, A. Doller, A. Babelova, W. Tsalastra, K. Moreth, L. Schaefer, J. Pfeilschifter, W. Eberhardt, Molecular mechanisms of TGF beta receptor-triggered signaling cascades rapidly induced by the calcineurin inhibitors cyclosporin A and FK506, J. Immunol. 181 (4) (2008) 2831–2845.

[70] Q. Xiao, Y. Guan, C. Li, L. Liu, D. Zhao, H. Wang, Decreased expression of transforming growth factor-β1 and α-smooth muscle actin contributes to the protection of lotensin against chronic renal failure in rats, Ren. Fail. 40 (1) (2018) 583–589.

[71] V. Masola, A. Carraro, S. Granata, L. Signorini, G. Bellin, P. Violi, A. Lupo, U. Tedeschi, M. Onisto, G. Gambaro, G. Zaza, In vitro effects of interleukin (IL)-1 beta inhibition on the epithelial-to-mesenchymal transition (EMT) of renal tubular and hepatic stellate cells, J. Transl. Med. 17 (1) (2019) 12.

[72] C.-L. Yen, Y.-J. Li, H.-H. Wu, C.-H. Weng, C.-C. Lee, Y.-C. Chen, M.-Y. Chang, T.-H. Yen, H.-H. Hsu, C.-C. Hung, C.-W. Yang, Y.-C. Tian, Stimulation of transforming growth factor-beta-1 and contact with type I collagen cooperatively facilitate irreversible transdifferentiation in proximal tubular cells, Biomed. J. 39 (1) (2016) 39–49.

[73] M. Forino, R. Torregrossa, M. Ceol, L. Murer, M. Della Vella, D. Del Prete, A. D'Angelo, F. Anglani, TGFbeta1 induces epithelial-mesenchymal transition, but not myofibroblast transdifferentiation of human kidney tubular epithelial cells in primary culture, Int. J. Exp. Pathol. 87 (3) (2006) 197–208.

[74] J. Bariety, G.S. Hill, C. Mandet, T. Irinopoulou, C. Jacquot, A. Meyrier, P. Bruneval, Glomerular epithelial-mesenchymal transdifferentiation in pauci-immune crescentic glomerulonephritis, Nephrol. Dialysis Transpl. 18 (9) (2003) 1777–1784.

[75] M. Fragiadaki, R.M. Mason, Epithelial-mesenchymal transition in renal fibrosis Evidence for and against, Int. J. Exp. Pathol. 92 (3) (2011) 143–150.

[76] I. Loeffler, G. Wolf, Epithelial-to-Mesenchymal Transition in Diabetic Nephropathy: Fact or Fiction? Cells 4 (4) (2015) 631–652.

[77] M. Camici, F. Galetta, N. Abraham, A. Carpi, Obesity-related glomerulopathy and podocyte injury: A mini review, Front Biosci (Elite Ed) 4 (2012) 1058–1070.

[78] M.E. Hall, J.M. do Carmo, A.A. da Silva, L.A. Juncos, Z. Wang, J.E. Hall, Obesity, hypertension, and chronic kidney disease, Int. J. Nephrol. Renovascular Disease 7 (2014) 75–88.

[79] M. Spencer, L. Yang, A. Adu, B.S. Finlin, B. Zhu, L.R. Shipp, N. Rasouli, C. A. Peterson, P.A. Kern, Pioglitazone Treatment Reduces Adipose Tissue Inflammation through Reduction of Mast Cell and Macrophage Number and by Improving Vascularity, PLoS One 9 (7) (2014), e102190.

[80] T. Qi, Y. Chen, H. Li, Y. Pei, S.L. Woo, X. Guo, J. Zhao, X. Qian, J. Awika, Y. Huo, C. Wu, A role for PFKFB3/iPFK2 in metformin suppression of adipocyte inflammatory responses, J. Mol. Endocrinol. 59 (1) (2017) 49–59.

[81] Y. Miyazaki, M. Matsuda, R.A. DeFronzo, Dose-response effect of pioglitazone on insulin sensitivity and insulin secretion in Type 2 Diabetes, Diabetes Care 25 (3) (2002) 517–523.

[82] R. Giannarelli, M. Aragona, A. Coppelli, S. Del Prato, Reducing insulin resistance with metformin: the evidence today, Diabetes Metab 29(4 Pt 2) (2003) 6s28-35.

[83] H. Yokoe, F. Yuasa, R. Yuyama, K. Murakawa, Y. Miyasaka, S. Yoshida, S. Tsujimoto, T. Sugiura, T. Iwasaka, Effect of pioglitazone on arterial baroreflex sensitivity and sympathetic nerve activity in patients with acute myocardial infarction and type 2 diabetes mellitus, J. Cardiovasc. Pharmacol. 59 (6) (2012) 563–569.

[84] D. Manzella, R. Grella, K. Esposito, D. Giugliano, M. Barbagallo, G. Paolisso, Blood pressure and cardiac autonomic nervous system in obese type 2 diabetic patients: Effect of metformin administration*, Am. J. Hypertens. 17 (3) (2004) 223–227.

[85] B. Brunmair, K. Staniek, F. Gras, N. Scharf, A. Althaym, R. Clara, M. Roden, E. Gnaiger, H. Nohl, W. Waldhäusl, C. Fürnsinn, Like Metformin Thiazolidinediones Inhibit Respiratory Complex I, A Common Mechanism Contributing to Their Antidiabetic Actions? 53 (4) (2004) 1052–1059.

[86] P. Breining, J.B. Jensen, E.I. Sundelin, L.C. Gormsen, S. Jakobsen, M. Busk, L. Rolighed, P. Bross, P. Fernandez-Guerra, L.K. Markussen, N.E. Rasmussen, J. B. Hansen, S.B. Pedersen, B. Richelsen, N. Jessen, Metformin targets brown adipose tissue in vivo and reduces oxygen consumption in vitro, Diabetes Obes. Metab. 20 (9) (2018) 2264–2273.

[87] J. Zhang, M. Fu, T. Cui, C. Xiong, K. Xu, W. Zhong, Y. Xiao, D. Floyd, J. Liang, E. Li, Selective disruption of PPARγ2 impairs the development of adipose tissue and insulin sensitivity, Proc. Natl. Acad. Sci. 101 (29) (2004) 10703–10708.

[88] P. Tontonoz, E. Hu, B.M. Spiegelman, Stimulation of adipogenesis in fibroblasts by PPARγ2, a lipid-activated transcription factor, Cell 79 (7) (1994) 1147–1156.

[89] S. Rizza, M. Cardellini, O. Porzio, C. Pecchioli, A. Savo, I. Cardolini, N. Senese, D. Lauro, P. Sbraccia, R. Lauro, M. Federici, Pioglitazone improves endothelial and adipose tissue dysfunction in pre-diabetic CAD subjects, Atherosclerosis 215 (1) (2011) 180–183.

[90] C. Sardu, N. D'Onofrio, M. Torella, M. Portoghese, F. Loreni, S. Mureddu, G. Signoriello, L. Scisciola, M. Barbieri, M.R. Rizzo, M. Galdiero, M. De Feo, M. L. Balestrieri, G. Paolisso, R. Marfella, Pericoronary fat inflammation and Major Adverse Cardiac Events (MACE) in prediabetic patients with acute myocardial infarction: Effects of metformin, Cardiovasc. Diabetol. 18 (1) (2019) 126.

[91] C. Sardu, P. Paolisso, C. Sacra, C. Mauro, F. Minicucci, M. Portoghese, M.R. Rizzo, M. Barbieri, F.C. Sasso, N. D'Onofrio, M.L. Balestrieri, P. Calabrò, G. Paolisso, R. Marfella, Effects of Metformin Therapy on Coronary Endothelial Dysfunction in Patients With Prediabetes With Stable Angina and Nonobstructive Coronary Artery Stenosis: The CODYCE Multicenter Prospective Study, Diabetes Care 42 (10) (2019) 1946–1955.

[92] J. Voelker, P.H. Berg, M. Sheetz, K. Duffin, T. Shen, B. Moser, T. Greene, S. S. Blumenthal, I. Rychlik, Y. Yagil, P. Zaoui, J.B. Lewis, Anti-TGF-β1 antibody therapy in patients with diabetic nephropathy, J. Am. Soc. Nephrol. : JASN 28 (3) (2017) 953–962.

[93] K. Tanabe, Y. Maeshima, Y. Sato, J. Wada, Antiangiogenic Therapy for Diabetic Nephropathy, BioMed research international 2017 (2017) 5724069-5724069.